

Trabajo de Fin de Grado

Synthesis and characterization of a metal-organic framework

Eva Cerviño Luridiana

Grado en Física

Curso 2021-2022

Tutor: Jorge Pasán García

Cotutor: Raúl González Martín

AGRADECIMIENTOS

A todos los profesores, compañeros, familiares y amigos que me han ayudado en el Grado, especialmente a Anna y Esther, por hacer estos años (y esta carrera) un poco más soportables; a mamá, por el amor y la paciencia que sólo puede dar una madre abnegada; y a papá, por enseñarme que lo único que puede rodar son las ruedas... o una persona rodando.

CONTENTS

Abstract	4
1. Introduction	5
1.1. Contaminants of Emerging Concern	5
1.2. Metal-organic frameworks (MOFs)	7
1.2.1. Zn(II)-triazole based MOFs: structural details	8
1.2.2. Synthesis of MOFs	9
1.2.3. Characterization of MOFs	9
1.3. Application of MOFs as sorbents in analytical microextraction techniques for the monitorization of CECs	10
2. Objectives	13
3. Experimental section	14
3.1. Materials and reagents	14
3.2. Synthesis of MOFs	15
3.3. Characterization of MOFs	16
3.3.1. X-ray diffraction	16
3.3.2. Thermal analysis	18
3.3.3. Gas adsorption	19
3.4. Analytical screening of MOFs	21
3.4.1. μ -dSPE with MOFs as sorbents	21
3.4.2. Chromatographic analysis	23
4. Results and discussion	26
4.1. Synthesis	26
4.2. Characterization of MOFs	28
X-ray diffraction.	28
Thermal analysis.	29
Gas adsorption.	31
4.3. Analytical performance	32
Conclusions	36
References	37

ABSTRACT

Este Trabajo de Fin de Grado se ha realizado en colaboración con el grupo de investigación multidisciplinar de la Universidad de La Laguna “Materiales para Análisis Químico” (MAT4LL), especializado en el diseño de novedosos materiales para el desarrollo de métodos de extracción de compuestos de interés en muestras de diferente naturaleza, especialmente medioambientales y biológicas. Entre las aplicaciones analíticas en las que el grupo posee mayor experiencia destaca la monitorización de contaminantes emergentes.

En este Trabajo de Fin de Grado, se han sintetizado dos redes metal-orgánicas (MOFs) basados en Zn(II) y triazol mediante el método solvotermal y se han determinado sus principales propiedades físicas mediante una serie de técnicas de caracterización. La estructura cristalina del MOF ha sido determinada mediante difracción de rayos X; su estabilidad térmica, mediante un análisis termogravimétrico, y su superficie específica y porosidad mediante una prueba de adsorción de gases. Tras la caracterización, se ha determinado su capacidad para extraer una serie de CECs de una disolución acuosa mediante el método de extracción en fase sólida dispersiva miniaturizada (μ -dSPE), en combinación con cromatografía líquida de ultra alta resolución con detección UV-Visible (UHPLC-UV).

Se han obtenido cristales planos de pequeño tamaño. La calidad de los difractogramas de la prueba de rayos X realizadas confirman su carácter altamente cristalino. Ambos compuestos son térmicamente estables hasta los 350 °C y tienen una superficie específica de 20 m²/g y 200 m²/g.

La capacidad del MOF para la extracción y preconcentración de los CECs estudiados es notablemente alta, varía entre el 50% y el 100%, dependiendo del contaminante, y es mejor para moléculas polares de pequeño tamaño. Se han comparado los resultados con los obtenidos con otros MOFs sintetizados en estudios anteriores, y se ha concluido que los compuestos sintetizados demuestran un buen perfil extractivo en comparación con otros MOFs de la misma familia.

1. INTRODUCTION

En esta sección se explica qué son los contaminantes emergentes, sus potenciales riesgos sobre la salud humana y las posibles aplicaciones de las redes metal-orgánicas (MOFs) para el monitoreo de la presencia de estos contaminantes en el ambiente. Se explica qué son los MOFs y sus principales propiedades y características estructurales. Se describen los MOFs pertenecientes a la familia del Zn(II)-triazol y se explican los pasos relativos a la síntesis, caracterización y evaluación de los MOFs como extractores de contaminantes.

1.1. CONTAMINANTS OF EMERGING CONCERN

Contaminants of Emerging Concern (CECs) are chemical products present in the environment whose potential risks to human health and ecosystems are currently being studied. It is important to stress that they are not necessarily newly introduced contaminants: they are termed “emergent” because their negative impact on both human health and environment has only recently been discovered^[1]. CECs span a wide variety of natural and anthropogenic substances and their by-products, such as drugs, artificial sweeteners, pesticides, microplastics, pharmaceuticals and personal care products (PPCPs). Table 1 includes representative examples of each group of CECs, together with some of their negative effects in the human health and the environment.

Among CECs, PPCPs are receiving increasing attention, both because of the magnitude of their consumption (and, therefore, the continuous introduction of contaminants into the environment) and because of the general lack of regulation regarding the maximum levels of these contaminants in the environment that do not provoke risks for human health. PPCPs are often disposed of in municipal wastewater and, when not effectively treated, end up in river and lake waters and reach groundwater, our drinking water supply. Many of these PPCPs can act as endocrine disruptors, capable of altering the human body's hormonal system. Chronic exposure to these pollutants may lead to an increased risk of cancer, obesity, decreased fertility, or neurodevelopmental disorders^{[2][3][4]}.

CECs contamination is a growing problem that is becoming increasingly difficult to control, as the current global production and consumption levels involve, among other issues, a continuous generation of waste. Therefore, the need to develop techniques to monitor CECs

is of rising importance, and several methods to prevent or limit their presence in the environment are currently being studied. In this sense, it is important to highlight the increasing use of sorbents that can extract CECs present at very low concentrations in environmental samples, which allow the subsequent analytical determination of those contaminants. Among the most studied sorbents, metal-organic frameworks (MOFs) have been suggested as good candidates to extract some CECs, especially PPCPs, from wastewater.

Category	Examples	Potential health effects
Pharmaceuticals	antibiotics (e.g., ciprofloxacin), painkillers (e.g., ibuprofen), antidepressants (e.g., fluoxetine)	genotoxicity (DNA damage), endocrine disruption, developmental delays, organ damage, antibiotic resistance
Personal Care Products	musks and fragrances (e.g., galaxolide), preservatives (e.g., parabens), UV filters (e.g., octinoxate)	altered gene expression, endocrine disruption, antibiotic resistance, genotoxicity (DNA damage)
Food additives	caffeine, nicotine, artificial sweeteners (e.g., sucralose, saccharin, aspartame)	genotoxicity (DNA damage), impaired reproduction, inhibited or altered growth
Pesticides	herbicides (e.g., atrazine)	endocrine disruption, immunosuppression
Industrial Chemicals	organic solvents (e.g., 1,4-dioxane), plastic formation (e.g., bisphenol A)	increased mortality, bioaccumulation in tissues
Disinfection by- products	disinfection by-product from water treatment (dihalobenzoquinones, Iodotrihalomethanes)	cytotoxicity (cell damage), genotoxicity (DNA damage), carcinogenesis
Microplastics	polyethylene, polystyrene, nylon, polyester, polypropylene	endocrine disruption, reduced growth, reduced reproduction

Table 1. Summary of main CECs categories, examples, and potential health effects. Data has been obtained from references (5) and (6).

1.2. METAL-ORGANIC FRAMEWORKS (MOFs)

MOFs are crystalline structures consisting of metal ions and organic ligands. The metal ions form nodes that link the ligands arms to form a porous structure with an extraordinarily large surface area, which makes these materials promising candidates to efficiently trap target compounds on their pores. By using different metal atoms and organic linkers, the pore size and chemical functionality of the MOFs surfaces, and thus the adsorption properties against various chemical species, can be tuned. These two characteristics —high surface area and tunable porosity— make MOFs extremely interesting in a wide variety of applications, such as gas storage and separation, liquid separation and purification, catalysis, drug delivery and adsorption removal of CECs.

Table 2 shows several examples of different MOFs already used in the literature. The most employed ligands are 1,2,4-triazole and 1,4-benzenedicarboxylic acid and their amino derivatives, in combination with a zinc nitrate salt. The crystalline structure of the first two, CIM-81 (Canary Islands Material 81) and Reference substance 1 (Ref. 1), are shown in Figure 1.

MOF	Organic ligand(s)	Metal salt	References
Reference substance 1 (Ref. 1)	1,2,4-triazole and 2,6-naphthalenedicarboxylic acid	Zn(II) nitrate salt	(7)
CIM-81	1,2,4-triazole and 1,4-benzenedicarboxylic acid	Zn(II) nitrate salt	(8), (9)
CIM-82	2-amino-1,2,4-triazole and 1,4-benzenedicarboxylic acid	Zn(II) nitrate salt	(8), (9)
CIM-83	3-amino-1,2,4-triazole and 1,4-benzenedicarboxylic acid	Zn(II) nitrate salt	(8), (9)

Table 2. Some of the MOFs used in literature.

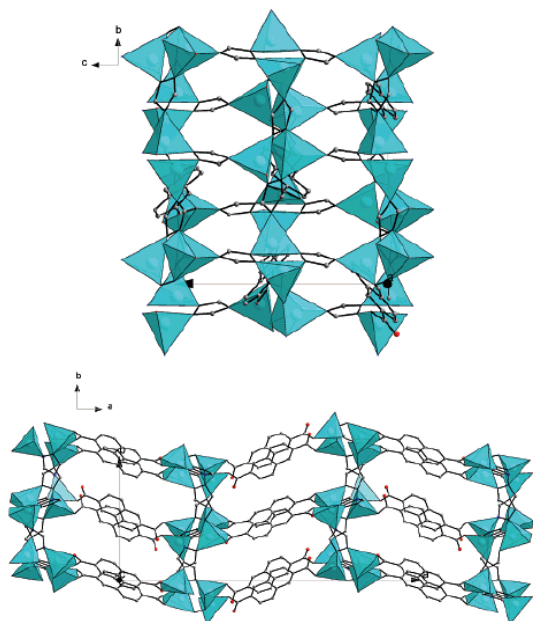


Figure 1(a). Crystal structure of Ref. 1 viewed from the a axis (top) and the c axis (bottom). Reference: (7).

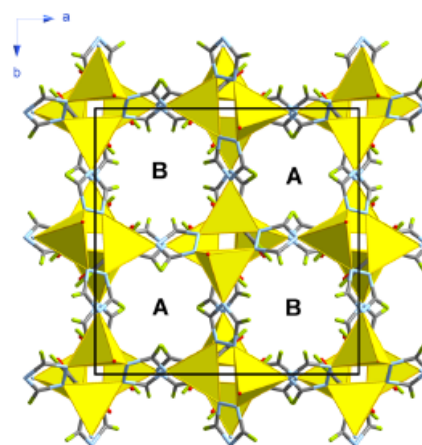


Figure 1(b). Crystal structure of CIM81 viewed from the c axis. Reference: (8).

1.2.1. ZN(II)-TRIAZOLE BASED MOFs: STRUCTURAL DETAILS

As mentioned above, by changing the organic ligands and nodes, an immense number of MOFs with different physical properties can be obtained. One of the most widely used techniques for MOF design, due to its practicality and ease of use, is the “pillared-layered” strategy, which consists in joining layers of a two-dimensional compound with an organic ligand to create a three-dimensional structure. MOFs created with this technique are called pillar-layered MOFs.

Within this type of MOFs, pillar-layered Zn(II)-triazole MOFs, consisting of layers of Zn-triazole moieties pillared by an organic ligand, have demonstrated promising physical properties, such as high gas uptake^{[9][10][11]}, adequate stability^[9], and better extraction capacity than other MOFs that have been subjected to the same experiments^[9].

In the study of MOFs, three parts should be considered: synthesis, characterization (i.e., the measurement and determination of their main physical properties), and analytical performance, (i.e., the study of the applicability of MOFs, either as adsorptive removers or as extractants of contaminants). Each of these steps is described in more detail in the following sections of this chapter.

1.2.2. SYNTHESIS OF MOFs

MOFs are usually synthesized by the solvothermal method. In this type of synthesis, the organic linker and the metal salt are dissolved in a solvent in a closed container and then temperatures above the boiling point of the solvent are applied, which generates an increase in pressure inside the recipient and facilitates the interaction between the reactants during the synthesis process. Some of the most common solvents employed for synthesizing MOFs are dimethylformamide (DMF), methanol, ethanol, and acetonitrile^{[12][13][14]}. Applied temperatures are typically between 80 °C and 180 °C^{[15][16]}, and the times of synthesis vary from several hours to several days^{[12][15]}.

1.2.3. CHARACTERIZATION OF MOFs

The characterization of MOFs can be performed by different physical tests depending on the research objectives. Three of the most common tests are X-ray diffraction, thermal analysis, and gas adsorption testing ^[12].

1.2.3.1. X-ray diffraction

X-ray diffraction studies and measures the interaction effects between an X-ray beam and a crystalline material. Analysis of X-ray diffraction data allows the determination of the crystal structure of the analyzed compound.

There are two main types of diffraction: powder XRD (X-Ray Diffraction) and Single-Crystal Diffraction. Single-Crystal Diffraction studies the structure within a single crystal, which does not necessarily represent the majority of the material; whereas powder XRD examines a large sample of polycrystalline material and provides information about the phase and crystallinity of the whole material.

The result of an X-ray diffraction experiment is a diffraction pattern (i.e., a curve with a series of peaks indicating the variation of the intensity of the diffracted radiation as a function of the diffraction angle). The position of the peaks, related to the crystallographic axes, gives information about the unit cell; while the intensity of the peaks (i.e., the amount of radiation reflected at given diffraction angles) shows information about atomic positions within the unit cell.

1.2.3.2. Thermal analysis

Thermal analysis encompasses a group of techniques in which a physical property of a material is measured as a function of temperature (or time) while the sample is subjected to a controlled and programmed heat treatment.

Thermogravimetric analysis (TGA) measures changes in the weight material of study as a function of temperature in a controlled atmosphere. Its main application is the study of thermal stability and related degradation mechanisms.

Differential Scanning Calorimetry (DSC) measures the difference in energy that a given sample must absorb or release to remain at the same temperature of a reference material during a controlled temperature program. Through DSC, the temperatures or temperature ranges at which transitions occur in the sample and the energies associated with them can be determined.

The result of thermal analysis is a set of three curves, TG, DTG, and DSC, which represent, respectively, the amount of mass lost versus temperature, the rate of mass decomposition versus temperature, and the difference in heat flux between sample and reference versus temperature.

The main rationale for thermal analysis is the evaluation of the overall stability of a MOF versus temperature and the determination of the temperature at which the material starts to decompose. This information is essential to determine the possible practical applications of the synthesized compounds.

1.2.3.3. Gas adsorption

Physical adsorption is a phenomenon in which the surface of a solid substance, called an adsorbent, fixes molecules from a gas or liquid phase with which it is in contact through Van der Waals-type intermolecular interactions. Through physical adsorption of gases, average values of properties of porous solids such as mean pore radius can be quantified. In general, the most important result of a gas adsorption test is the *adsorption isotherm*.

An adsorption isotherm is a curve that describes the amount of adsorption at a given relative pressure and constant temperature. According to IUPAC, there are six different types of adsorption isotherms, whose shape depends on the adsorbent's nature and the affinity of the adsorbate for the adsorbent. By evaluating this curve, parameters such as surface area or total pore volume, essential for the posterior analysis of pollutant adsorption results and the characterization of new MOFs, can be determined.

1.3. APPLICATION OF MOFs AS SORBENTS IN ANALYTICAL MICROEXTRACTION TECHNIQUES FOR THE MONITORIZATION OF CECs

In general, any analytical chemistry method can be divided into three stages: sampling, sample preparation, and analysis. Among these three steps, sample preparation is particularly well known for being the one that generates the greatest amounts of waste. Despite of that, it is the most important step in the analytical procedure, as it ensures the compatibility of the sample to be analyzed with analytical instrumentation, reducing or eliminating interferences that may hinder its detection. Thus, in recent years, attempts have been made to redesign many of the traditional sample preparation methods to minimize the contamination they produce^[8]^[9].

On this basis, *microextraction techniques* have been developed. In microextraction techniques, the extraction time and amount of extraction material used for sample preparation are significantly reduced compared to traditional extraction methods. There are several types of microextraction techniques, depending on the liquid or solid nature of the extraction material and the mechanism followed to expose the sample to the extractant. Some examples of microextraction techniques are liquid-phase microextraction (LPME)^[17], and micro-dispersive solid-phase extraction (μ -dSPE)^[9].

MOFs have been especially successful as sorbents in μ -dSPE. The most conventional μ -dSPE procedure involves two steps: extraction and desorption.

In the extraction step, small amounts of MOF (typically ~500 mg) are added to a liquid sample containing the analytes to be extracted and then the sample is stirred to favor the contact between the MOF and the analytes. Once the dispersion process is completed, the two phases (the MOF with the extracted analytes and the solution with the remaining analytes) are separated by centrifugation.

Once the extraction step is complete, the desorption step can be performed: the supernatant is discarded, and MOF is treated with a desorption solvent that dissolves the desorbed analytes from the MOF. As in the extraction step, the solution is stirred and centrifuged. The desorption solvent is then filtered, evaporated, and reconstituted in a smaller volume of solvent to ensure the compatibility with the analytical determination system.

As mentioned, MOFs can be promising candidates for the extraction of CECs in wastewater. To determine the effectiveness of a MOF as extractant for a group of CECs in a μ -

dSPE procedure, both its adsorption capacity and its ability to preconcentrate should be evaluated. Preconcentration is usually needed in analytical extraction techniques as the contaminants are at very low levels in the environment, thus being impossible their direct determination considering the limitation of sensitivity of the most common detection systems. In consequence, MOFs should be able to extract target compounds from a large volume solution of a sample (usually 10 mL) in which they are at low concentration, and then they are desorbed into a smaller volume of solvent (at the microliters order), thus increasing their concentration, and making feasible their analytical determination.

To evaluate extraction and preconcentration capacity, two essential parameters must be determined: adsorption capacity and desorption capacity. Both capacities will depend on the MOF's structure, the CECs used, and the experimental conditions; and can be assessed through a series of experiments commonly referred to as *screening*.

Screening can be divided into an adsorption test and a desorption test, each of which has two stages: sample preparation, and chromatographic analysis.

In the sample preparation step, the MOF is added to an aqueous standard solution containing CECs at a certain concentration, to see how much it extracts; and then it is treated with a desorption solvent, which dissolves the extracted compounds after desorbing them from the MOF. Then, the remaining concentration of CECs in the aqueous standard after the extraction, as well as the concentration of the desorbed compounds, are obtained by chromatographic analysis, thus assessing the adsorption and desorption capacity of the MOF.

2. OBJECTIVES

El objetivo de este trabajo es sintetizar, caracterizar y evaluar como extractores de contaminantes dos MOFs pertenecientes a la familia del Zn(II)-triazol.

The general aim of this project is the synthesis and characterization of two pillared-layer Zn-triazolate metal-organic frameworks (MOFs), and the subsequent evaluation of their capacity as adsorbents of contaminants of emerging concern (CECs) from wastewater.

To achieve the general purpose of this work, two partial objectives are established:

- i) Synthesis of pillared-layer Zn-triazolate MOFs by a solvothermal approach, and characterization by X-ray diffraction, thermal analysis, and gas adsorption testing.
- ii) Analytical application of the synthesized MOFs: evaluation of the adsorption capacity of the MOFs towards a group of some CECs in a μ -dSPE method, using high-performance liquid chromatography with UV-Vis detection (HPLC-UV) as an analytical determination system.

3. EXPERIMENTAL SECTION

En esta sección se explican los procedimientos seguidos y la instrumentación utilizada en la síntesis y caracterización de los MOF y el estudio de adsorción de contaminantes.

3.1. MATERIALS AND REAGENTS

Tables 3 and 4 summarize the reagents used in the MOFs' synthesis and the selected PPCPs for the analytical screening. When accurate weight measures were required, a balance with a precision of 0.1 mg was used.

Reactants		
Name	Formula	Abbreviation
Zinc nitrate hexahydrate	$Zn(NO)_3 \cdot 6H_2O$	-
1,2,4-Triazole	$C_2H_3N_3$	TRZ
2,6-Naphthalenedicarboxylate	$C_{12}H_8O_4$	2,6-NDC
Azobenzene	$C_{12}H_{10}N_2$	AZBC
Dimethylformamide	C_3H_7NO	DMF

Table 4. Reactants used in MOFs' synthesis.

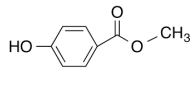
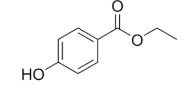
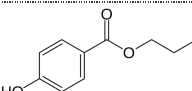
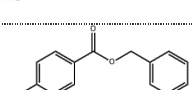
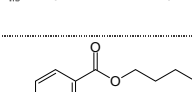
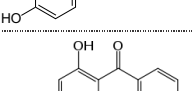
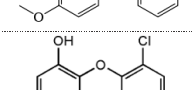
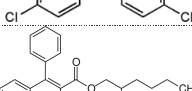
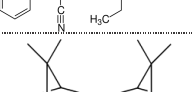
PPCPs						
Name	Structure	M.W. (g·mol ⁻¹)	Log K _{ow}	W.S. at 25 °C (mg·L ⁻¹)	pK _a (mol·L ⁻¹)	Reference
Methyl paraben (MPB)		152.15	1.66	2.5·10 ³	8.5	(18.1)
Ethyl paraben (EPB)		166.18	2.19	1.2·10 ³	8.3	(18.2)
Propyl paraben (PPB)		180.20	2.71	4·10 ³	8.5	(18.3)
Benzyl paraben (BzPB)		228.24	3.56	1.5·10 ³	8.2	(18.4)
Butyl paraben (BP)		194.23	3.24	13	8.5	(18.5)
Oxybenzone paraben (BP3)		228.24	3.64	13	7.1	(18.6)
Triclosan (Tr)		289.54	4.76	10	7.9	(18.7)
Octocrylene (OCR)		361.48	5.77	3.8	-	(18.8)
Camphor (MBC)		152.23	2.4	1.2	-	(18.9)

Table 4. PPCPs evaluated in the MOFs' screening, and their main properties. Pictures source: wikipedia.com

Legend: M.W.: Molecular Weight; S.W.: Solubility in Water; K_{ow}: octanol-water partition coefficient.

3.2. SYNTHESIS OF MOFs

Several batches of two zinc-based MOFs, compound **1** [Zn·(TRZ)·(2,6-NDC)·2DMF·2H₂O] and compound **2** [Zn·(TRZ)·(AZB)·2DMF·2H₂O] were synthesized following a solvothermal approach.

For all the synthesized MOFs, 1 mmol (297 mg) of zinc nitrate hexahydrate (Zn(NO₃)₆·6H₂O) and 1 mmol (70 mg) of 1,2,4-triazole (TRZ) were measured. Then, 0.5 mmols (108 mg) of 2,6-naphthalenedicarboxylate (2,6-NDC) were added to compound **1** batches and 0.5 mmols (91 mg) of laboratory-made azobenzene (AZB) to compound **2** batches.

Subsequently, 5 mL of DMF were added to each batch. The solution was transferred to a 23 mL vial, mixed for one hour on a magnetic stirrer or 15 minutes under sonication, heated at 130 - 150 °C for 3 days, washed with DMF, filtered, and dried at 70 °C for one hour. Figure 2 includes a scheme of the procedure followed for the solvothermal synthesis of the MOFs.

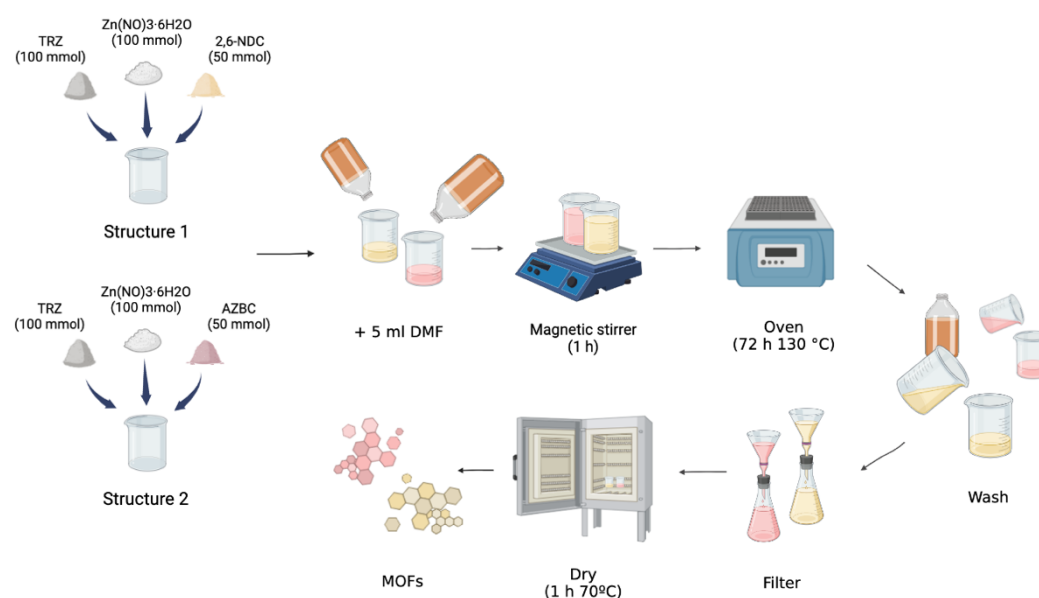


Figure 2. MOFs' synthesis process.

3.3. CHARACTERIZATION OF MOFS

3.3.1. X-RAY DIFFRACTION

Instrumentation. This experiment was carried out with the Malvern Panalytical's Empyrean diffractometer (Figure 3). The diffractometer consists of an X-ray tube and a detector screen that simultaneously rotate around the sample, which remains stationary. The rotation allows the sample to be irradiated at different angles, which are determined by a goniometer during the measurement.

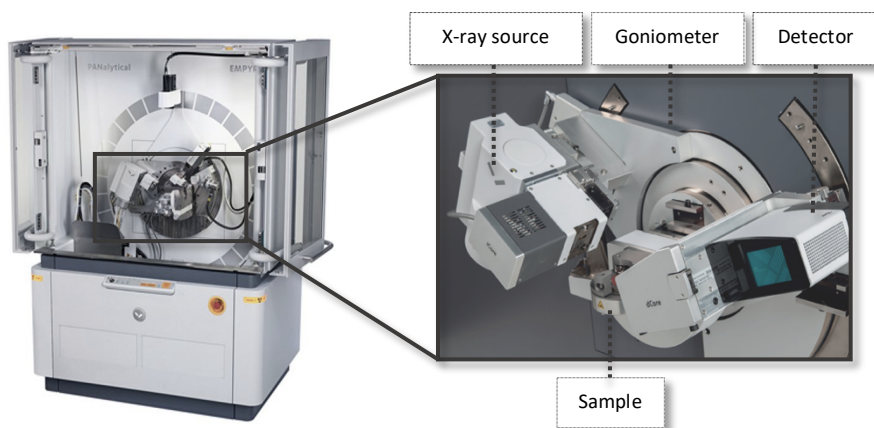


Figure 3. Malvern Panalytical's Empyrean X-ray diffractometer. Source: malvernpanalytical.com.

Operation. Approximately 150 mg of the MOF sample was reduced to powder with the help of a pestle and placed in a small disk-shaped container. The disk is placed on the sample holder of the diffractometer. The measurement is then started, and the X-ray tube and the detector screen are rotated around it. When the radiation emitted by the X-ray tube reaches the sample, the atoms of the analyzed powder act as a diffraction grating, producing bright spots at certain angles that are detected on the screen, as shown in the scheme of Figure 4. By measuring the angles 2θ at which these intensity maxima occur, the diffraction grating constant (and thus, the atomic spacing and crystal structure) can be determined by Bragg's law:

$$n\lambda = 2d \cdot \sin \theta, \quad (1)$$

where n is an integer, λ is the wavelength of the X-rays, d is the distance between the crystal lattice planes and θ , the angle between the incident rays and the scattering planes, corresponds to one half of the angle of each diffraction maxima.

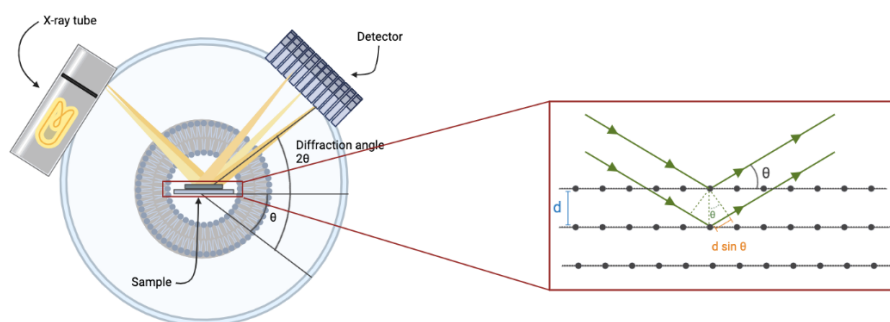


Figure 4. X-ray diffraction and Bragg's Law.

3.3.2. THERMAL ANALYSIS

Instrumentation. Thermal analysis was conducted using the Simultaneous Thermal Analyzer SDT-650 from TA Instruments (Figure 5), which performs DSC and TGA simultaneously. The main parts of the instrument are a microcomputer that allows control of the instrument, a furnace, a gas purge system, and a precision balance with two horizontal ceramic beams (for the sample and the reference) with an integrated thermocouple that provides direct sample and reference temperature measurements.

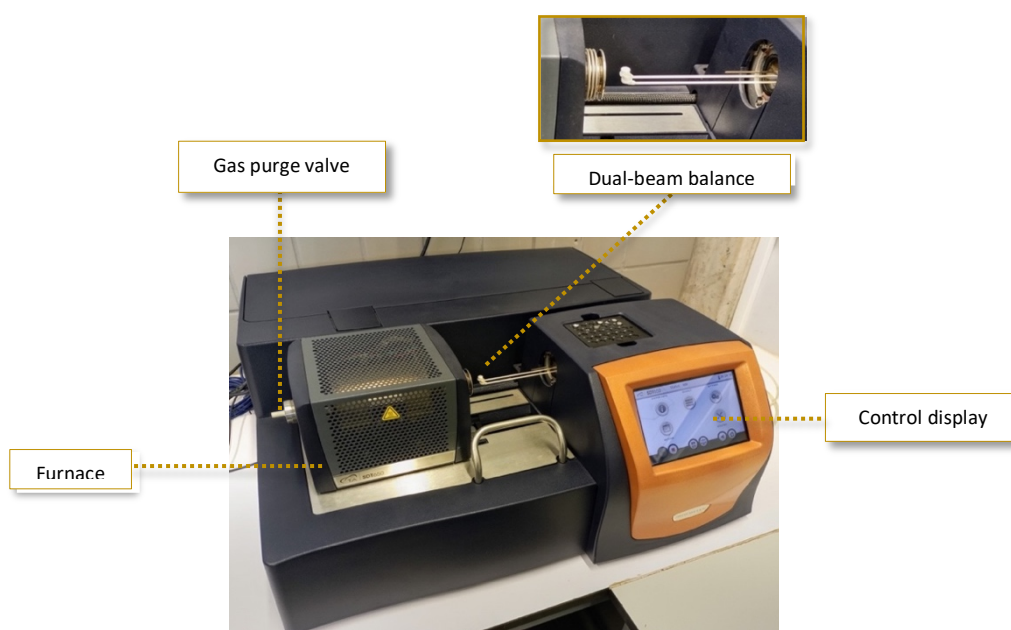


Figure 5. TA Instruments SDT-650 Thermal Analyzer.

Operation. 10 mg of MOF are measured and placed in the sample holders suitable for the chosen temperature program (aluminum, from room temperature – 600 °C, 10 °C/min). Test sample and reference sample are placed on the balance beams and the measurement is started. As the temperature program progresses, the balance detects the weight change of the sample, while the thermocouple measures the heat flux difference between the sample and the reference. Figure 6 shows a scheme of how the TG/DSC analysis works.

As stated in the introduction, the obtained data is displayed in three graphs: TG (weight change as a function of temperature), DTG (rate of weight loss as a function of temperature), and DSC (heat flow difference between sample and reference as a function of temperature). Dehydration or decomposition of the sample translates into a maximum in the DTG and a

decrease of the TG curve, whereas a maximum or a minimum in the DSC curve indicates a thermodynamical transition.

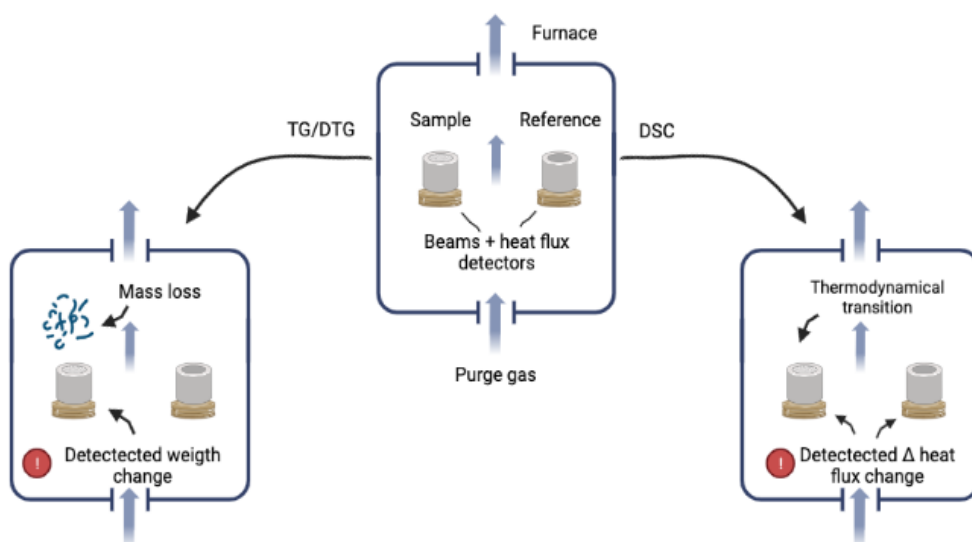


Figure 6. DSC and TG/DTG analysis.

3.3.3. GAS ADSORPTION

Instrumentation. The analysis instrument used is the Micromeritics ASAP 2020 (Figure 7), consisting of a control software, a cooling system, two vacuum pumps (*degas ports*) for the sample cleaning, and a gas pump (*analysis port*) for the adsorption test. The test was performed at at 77K in the $0.01 \leq P/P_0 \leq 0$ range.

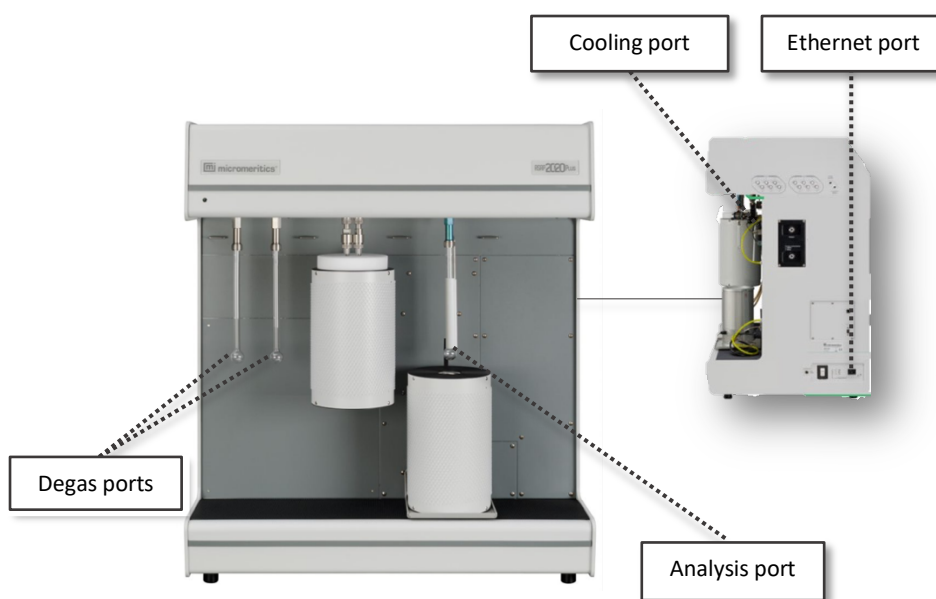


Figure 7. Micromeritics ASAP 2020 Adsorption Analyzer. Source: micromeritics.com.

Operation. 150 mg of MOF are measured and placed on a sample tube. The tube is placed on the *degas port* and the *degas program* is started. The degas program cleans the sample by bringing it under a vacuum at low temperatures, removing contaminants absorbed from exposure to the atmosphere.

The clean sample is loaded into the analysis port, from which controlled amounts of nitrogen are inoculated into the tube. After each dosage of gas, when the pressure reaches equilibrium, the amount of gas absorbed by the MOF is measured. The adsorbed gas data for each pressure at a constant temperature is plotted and an adsorption isotherm is obtained. Assuming the curve has the form of a *BET isotherm*:

$$\frac{1}{v \left(\frac{p_0}{p} \right) - 1} = \frac{c - 1}{v_m c} \left(\frac{p}{p_0} \right) + \frac{1}{v_m c}, \quad (2)$$

where p and p_0 are the equilibrium and saturation pressure of the adsorbates at the adsorption temperature, v is the amount of gas adsorbed, v_m the amount of nitrogen required to form a monolayer, and c is the *BET constant*; we know that, for small relative pressures ($0.05 \leq p/p_0 \leq 0.35$), $\left(v \left(\frac{p}{p_0} \right) - 1 \right)^{-1}$ and $\left(\frac{p}{p_0} \right)$ have a linear relationship from whose slope A , v_m can be determined as follows:

$$v_m = \frac{1}{A + 1} \quad (3)$$

The specific surface area can be then calculated as:

$$S_{BET} = \frac{v_m N s}{V a}, \quad (4)$$

where N is Avogadro's number, s the adsorbate adsorption cross-section, V the molar volume of the adsorbed gas, and a the mass of the solid sample or adsorbent. A scheme of this process is shown in Figure 8.

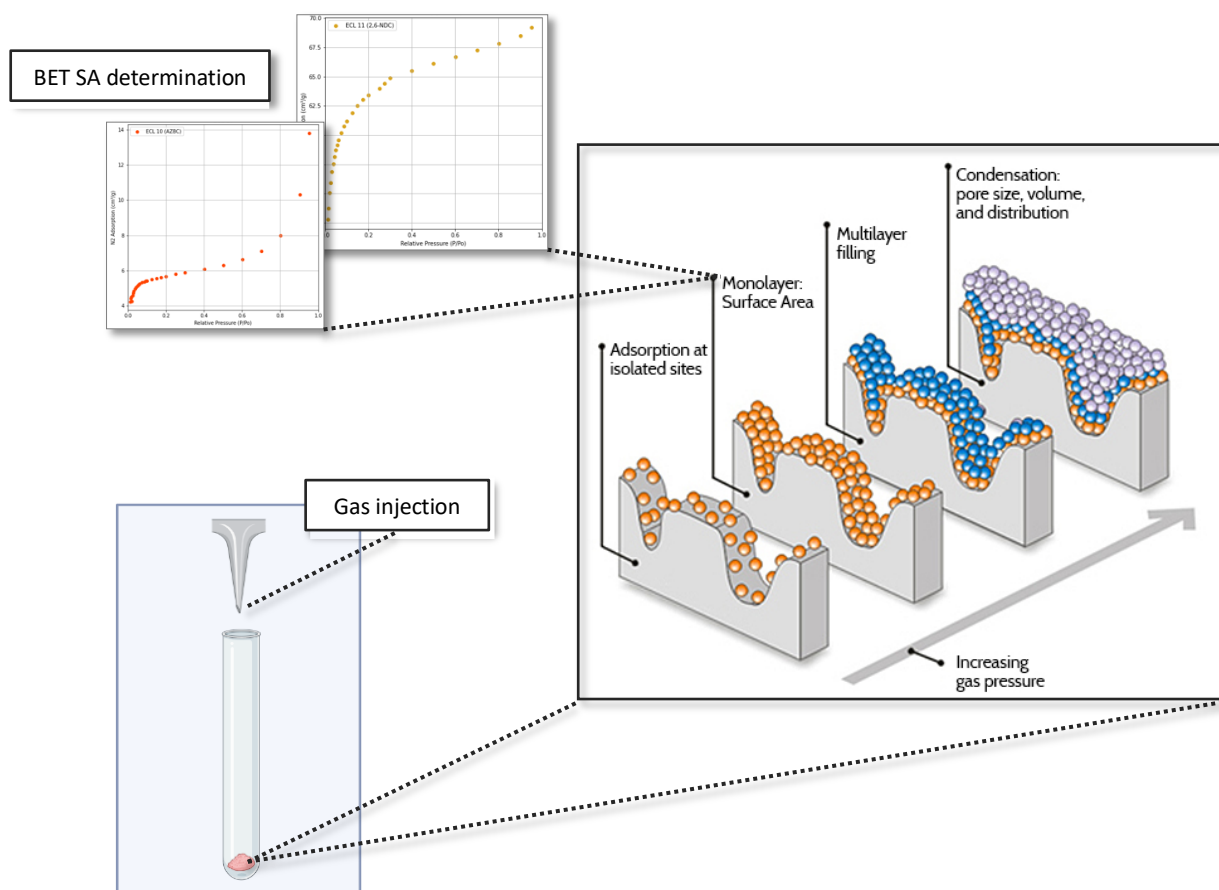


Figure 8. Adsorption analysis and BET Surface Area determination. Adsorption on surface picture source: psu.edu

3.4. ANALYTICAL SCREENING OF MOFs

To ensure the reliability and reproducibility of the results, the screening of each MOF is performed in triplicate.

3.4.1. μ -DSPE WITH MOFs AS SORBENTS

Instrumentation. For sample preparation, the following instruments were used: the Heidolph Multi Reax Top vortex for sample agitation, the Eppendorf 5720 centrifuge, and the IKA RV10 rotary evaporator with the VWR CVR 3000 vacuum controller, shown on Figure 9.



Figure 9. From left to right: Heidolph Multi Reax Top vortex, Eppendorf 5702 centrifuge, and IKA RV10 Rotary evaporator (source: imbm.co).

Operation of μ -dSPE. *Extraction step.* After washing and thermal activation, 20 mg of each MOF are weighed into a centrifuge tube and 10 mL of an aqueous solution standard with a concentration of $0.1 \mu\text{g}\cdot\text{mL}^{-1}$ of the selected PCPs at pH 5 are added. To ensure that the MOF interacts with the PPCPs, the sample is stirred for 3 minutes in the vortex and centrifugated at $2504 \times g$ for another 3 minutes. The supernatant is saved for further chromatographic analysis. Figure 10 shows a scheme of the experimental procedure followed.

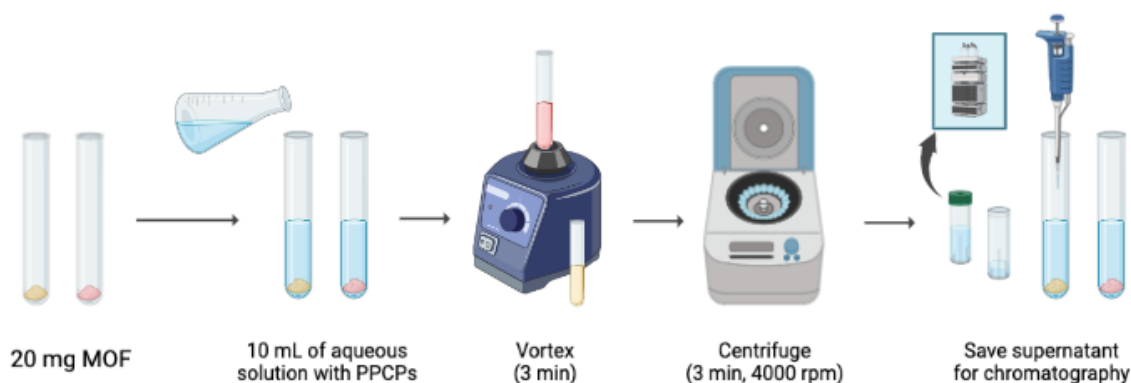


Figure 10. Extraction step of a μ -dSPE procedure with MOFs.

Desorption step. Once the supernatant is saved, the rest of the aqueous solution is discarded and 500 μL of acetonitrile are added to the MOF. The previous process is repeated: 3 minutes in the vortex and 3 minutes in the centrifuge at $2504 \times g$. The MOF is removed from the solution with a filter. The solvent is evaporated using a rotary evaporator and reconstituted

with 100 μL of an acetonitrile (ACN:H₂O) mixture. A scheme of the procedure is shown in Figure 11.

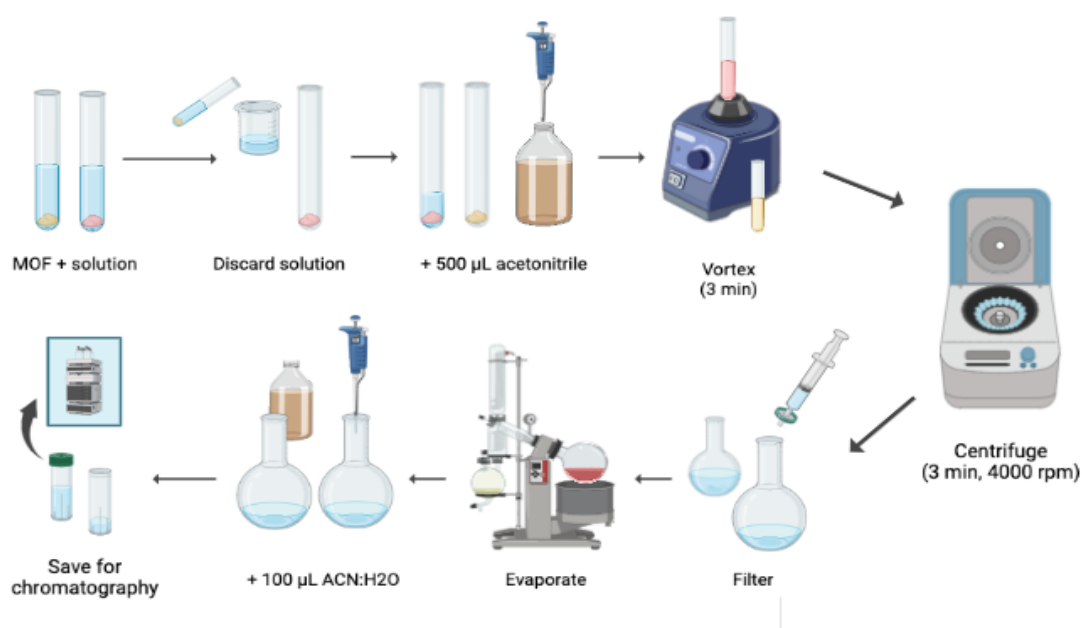


Figure 11. Desorption step of a μ -dSPE procedure with MOFs.

3.4.2. CHROMATOGRAPHIC ANALYSIS

The concentration of the CECs in each sample is determined by high-performance liquid chromatography with UV-Vis detection (HPLC-UV).

A chromatograph consists, essentially, of a column filled with a solid adsorbent material called the *stationary phase*, pumps that push a pressurized liquid solvent called the *mobile phase* containing the sample mixture through the column, and a detector that generates a signal proportional to the amount of sample component emerging from the column, resulting in a graph called *chromatogram*. In this work, the UHPLC 1260 Infinity Series chromatograph from Agilent Technologies was used, consisting of a quaternary pump, a Rheodyne 7725i injection valve, an InfinityLab Poroshell 120 EC-C18 column, a Varian ProStar 410 HPLC Autosampler, and a Vis-UV ProStar 325 LC Detector Series from Varian. Figure 12 shows a photo of the equipment.



Figure 12. UHPLC 1260 Infinity Series chromatograph, Varian ProStar 410 HPLC Autosampler, and Varian Vis-UV ProStar 325 LC Detector.

Determination of MOF extraction and preconcentration capacities. The data obtained in the chromatographic analysis is represented graphically in a *chromatogram*, a curve with a series of peaks corresponding to each of the compounds present in the solution. The position of the peaks on the horizontal axis identifies the compound (as it is influenced by the specific interaction of each compound with the stationary phase), while their area indicates the amount present in the solution. As stated in the introduction, the objective of the screening is to determine the extraction and preconcentration capacities of MOFs, for which it is necessary to evaluate two parameters.

Firstly, the *percentage of analyte or compound adsorbed by the material*, determined from the concentrations in CECs in the sample at the beginning and after the extraction test, is calculated.

Secondly, *the preconcentration and overall extraction capacity of the MOFs*, i.e., the capacity to adsorb and then desorb the analytes. To determine it, the peak areas of the chromatogram of the solution resulting from the desorption test are studied. As mentioned, those areas indicate the amount desorbed of each analyte.

High peak areas indicate that a large amount of the analyte has been adsorbed *and* desorbed. Low peak areas indicate either that the MOF does not have a good adsorption capacity (with the selected CECs), or that the MOF has a good adsorption capacity but no desorption capacity.

The higher the peak area, the more analyte the MOF can adsorb and desorb and the better its extraction and preconcentration capabilities.

By combining these two parameters (peak area and percentage of analyte extracted), we can therefore determine the adsorption and extraction capacity of the material.

4. RESULTS AND DISCUSSION

En esta sección se presentan los resultados obtenidos, se analizan, se discuten, y se comparan con otros resultados de la bibliografía.

4.1. SYNTHESIS

A total of 13 MOF batches were synthesized, six of compound **1** [Zn·(TRZ)·(2,6-NDC)·2DMF·2H₂O], and seven of compound **2** [Zn·(TRZ)·(AZB)·2DMF·2H₂O].

Plate-like and small-sized crystals were obtained (Figure 13). The experimental conditions and yield of each synthesis is reported in Table 5. Tables 6 and 7 compare the average yield and its standard deviation depending on the MOF (1 or 2) and the temperature at which they were heated. Cells with (-) correspond to MOFs whose synthesis was interrupted due to burning or contamination.

Batch	Organic ligand (2,6-NDC – AZBC)	Heating temperature (°C)	Yield (%)
1	2,6-NDC	150	56
2	AZBC	-	-
3	2,6-NDC	150	79
4	AZBC	150	76
5	AZBC	150	90
6	AZBC	130	-
7	AZBC	130	-
8	2,6-NDC	130	73
9	2,6-NDC	130	77
10	AZBC	130	88
11	2,6-NDC	130	52
12	AZBC	130	80
13	2,6-NDC	130	61

Table 5. Summary of synthesized MOFs, their experimental conditions, and yields.

Organic ligand	Average yield (%)	Standard deviation (%)
2,6-NDC	66	10
AZBC	84	6

Table 6. MOFs synthesis performance by organic ligand.

Temperature (°C)	Average yield (%)	Standard deviation (%)
130	75	6
150	72	6

Table 7. MOFs synthesis performance by temperature.

There are no notable differences between the batches heated at 130 °C and those heated at 150 °C in terms of crystal size or yield. However, compound **2** batches show, on average, higher yields, and larger crystal size than compound **1** batches.

Although not much research has been done on the causes and processes influencing crystal shape and size in the synthesis of MOFs^{[19][20]}, it is known that they depend on a wide number of factors, such as experimental technique, experimental conditions (e.g. heating rate, concentration, temperature...) and nature of the reagents^{[20][21]}.

In summary, for this experimental setup, there are no significant differences in the synthesis outcomes within the temperature range studied (130 °C - 150 °C) and the results in terms of crystal size and yield are better for compound **2** than for compound **1**. A change in the experimental conditions could lead to different results.

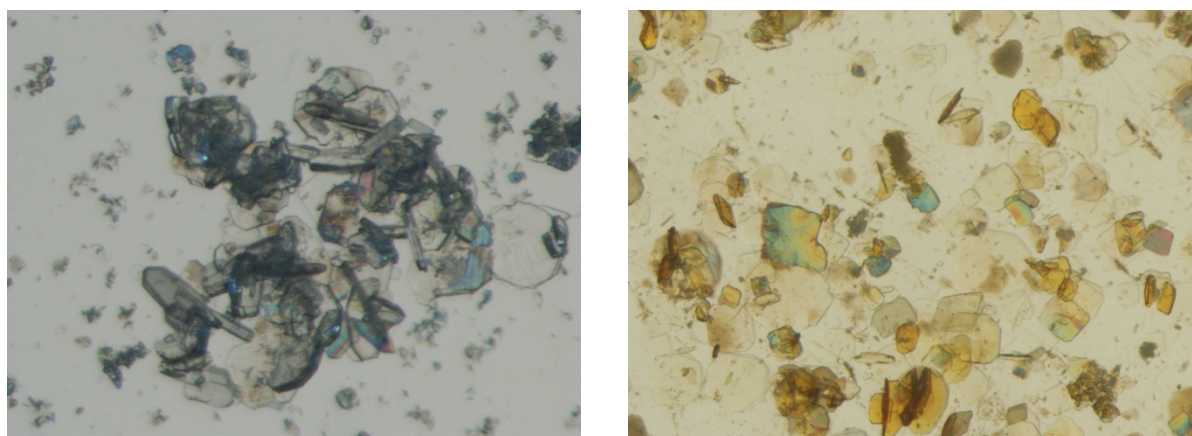


Figure 13. Microscope pictures of crystals of 1 (left) and 2 (right).

4.2. CHARACTERIZATION OF MOFs

X-RAY DIFFRACTION. X-ray diffraction has been performed on the 13 synthesized batches. Among all the spectra obtained, those of higher quality (i.e., better signal-to-noise ratio, narrower peaks) have been chosen for analysis and further testing. Figures 14 and 15 show the diffraction patterns of the MOFs' chosen batches.

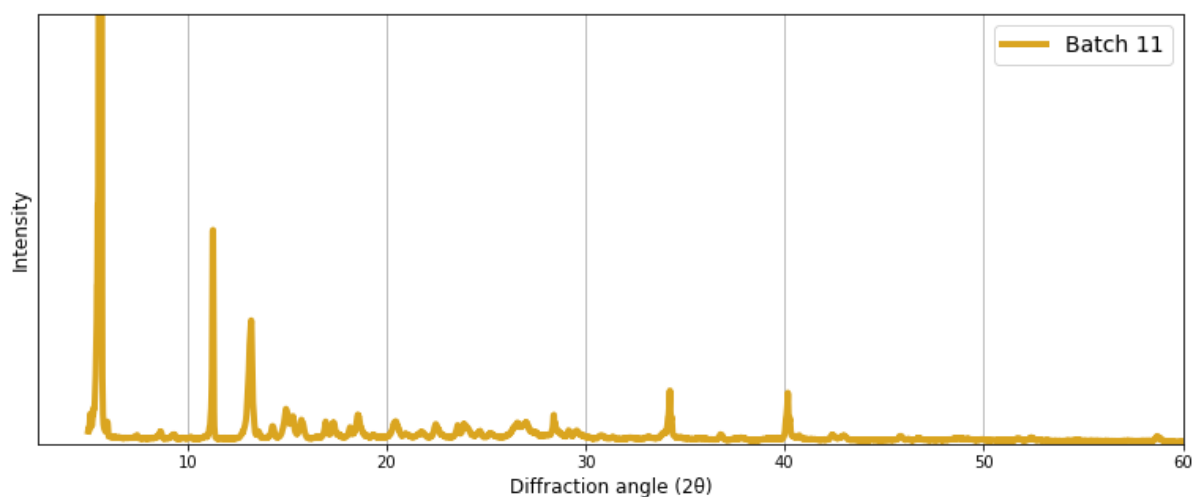


Figure 14. X-ray diffraction pattern (Compound 1— 2,6-NDC).

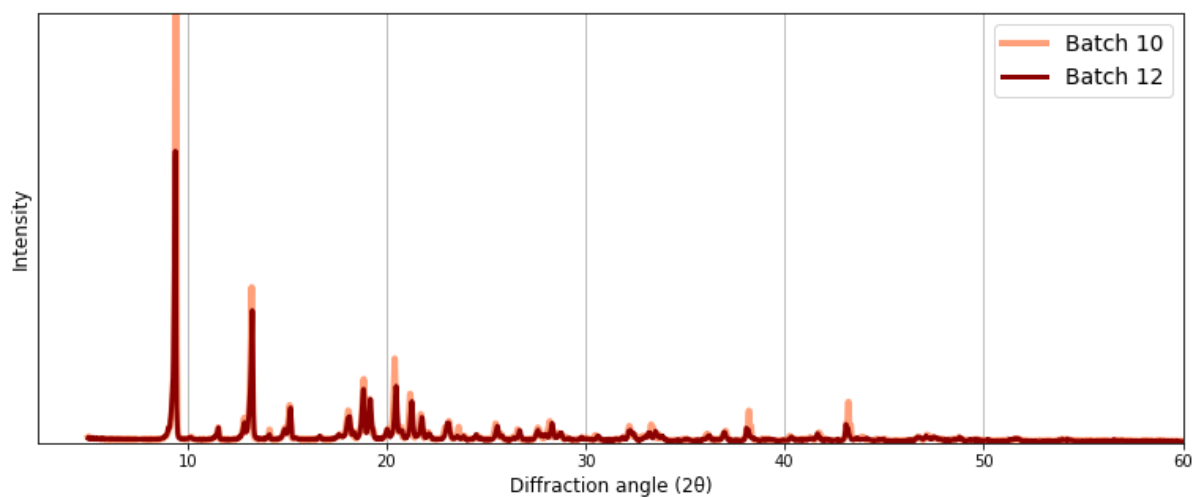


Figure 15. X-ray diffraction pattern (Compound 2— AZBC).

Compound 1 results can be compared with those of the reference in literature (7), to which we will refer, from now on, as **R1**. In both cases, the diffraction spectra show the maximum intensity at around $\theta = 3^\circ$ ($2\theta = 6^\circ$), followed by several peaks of decreasing

intensity, one at around $\theta = 5^\circ$, and two at around $\theta = 6^\circ$. In compound **1**, two other peaks are visible around $\theta = 17^\circ$ and $\theta = 20^\circ$. There is not **R1** data for angles greater than $\theta = 11^\circ$, but, based on the results, it can be assumed that they will have similar behavior and that compound **1** has been successfully synthesized.

THERMAL ANALYSIS. Thermogravimetric analysis of the selected compounds was performed after X-ray diffraction. The results obtained are shown in Figures 16 and 17:

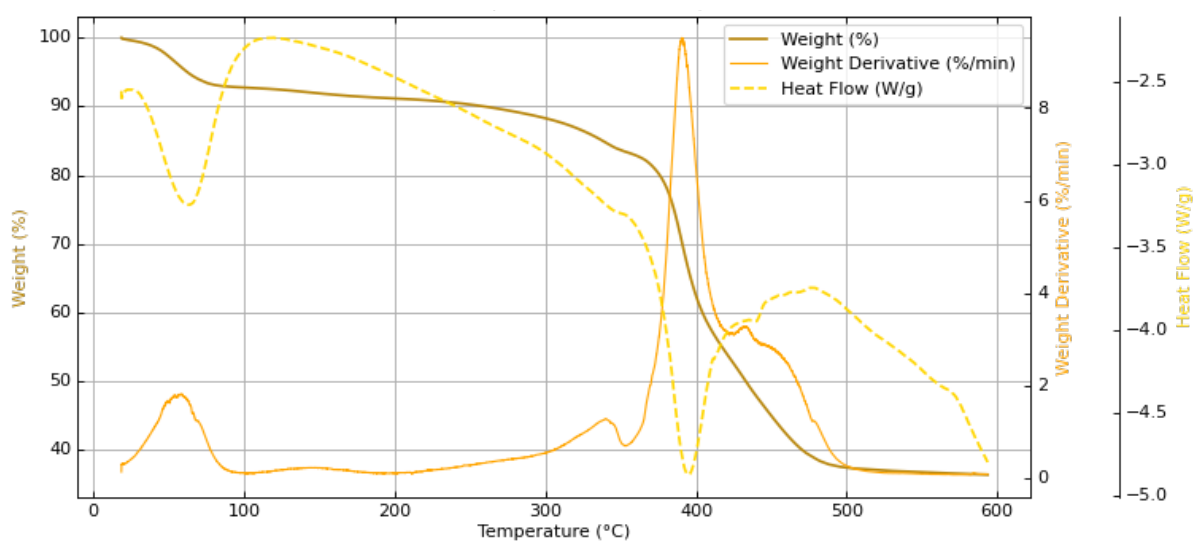


Figure 16. Thermal analysis curves: TG, DTG and DSC (Compound 1 — 2,6-NDC).

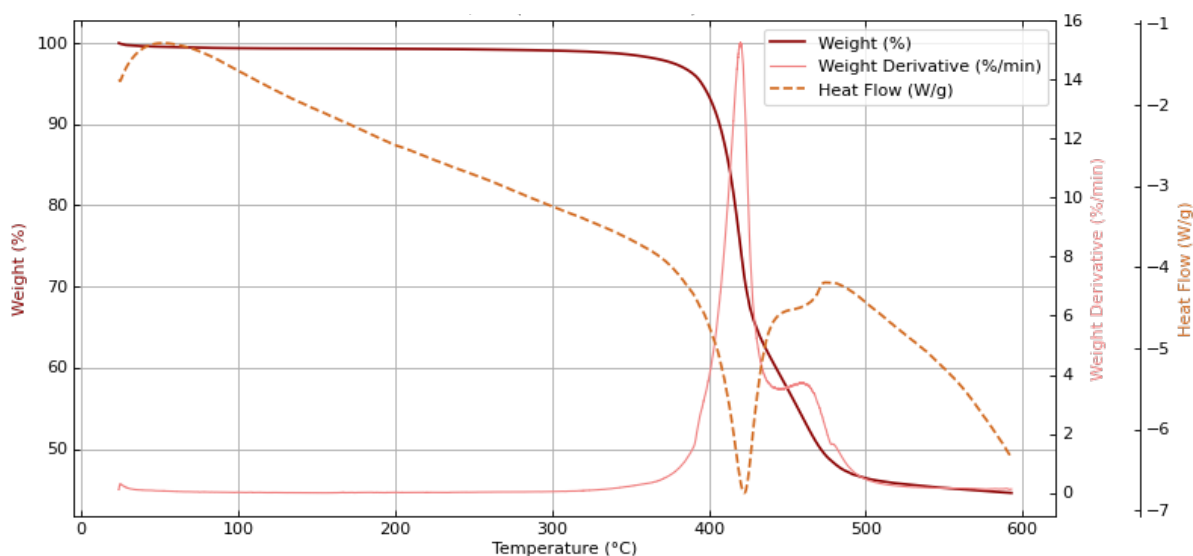


Figure 17. Thermal analysis curves: TG, DTG and DSC (Compound 2 — AZBC).

Compound **1** thermogram shows three stages of mass loss: the first two, around 50 °C and 320 °C, correspond to the evaporation of solvent molecules (respectively, acetone and DMF, which needs higher temperatures to evaporate because it is trapped inside the MOF). The third stage of mass loss corresponds to the decomposition of the material, which occurs between 375 °C and 500 °C and reaches the maximum weight loss rate at around 390 °C. From 400 °C onwards, the rate of decomposition begins to decrease, until it becomes practically nil from 500 °C onwards. In total, approximately 65% of the mass is lost.

This behavior is very similar to that obtained for **R1**: in both cases, it is possible to identify the acetone loss stage above 50 °C, the residual DMF molecule loss stage above 300 °C, and the decomposition stage above 400 °C. Moreover, in both thermograms, the decomposition rate of the compound reaches its maximum above 400 °C and decreases to zero above 500 °C. In the thermogram of the reference compound, the total decomposition of the compound is slightly higher: about 70%. A comparison of the TG curves of **1**, **2** and **R1** can be seen in Figure 18.

In compound **2** thermogram, hardly any mass loss is observed below 350 °C, indicating that almost no DMF or acetone was present. The compound starts to decompose at around 400 °C, reaches the maximum rate of decomposition at around 420 °C, and continues to decompose until around 500 °C. In total, compound **2** loses 45% of its mass.

We can conclude that compound **2** is the more thermally stable MOF of the two studied: not only is it the one that starts to decompose at the highest temperature, but it is also the one that decomposes the least at the end of the experiment.

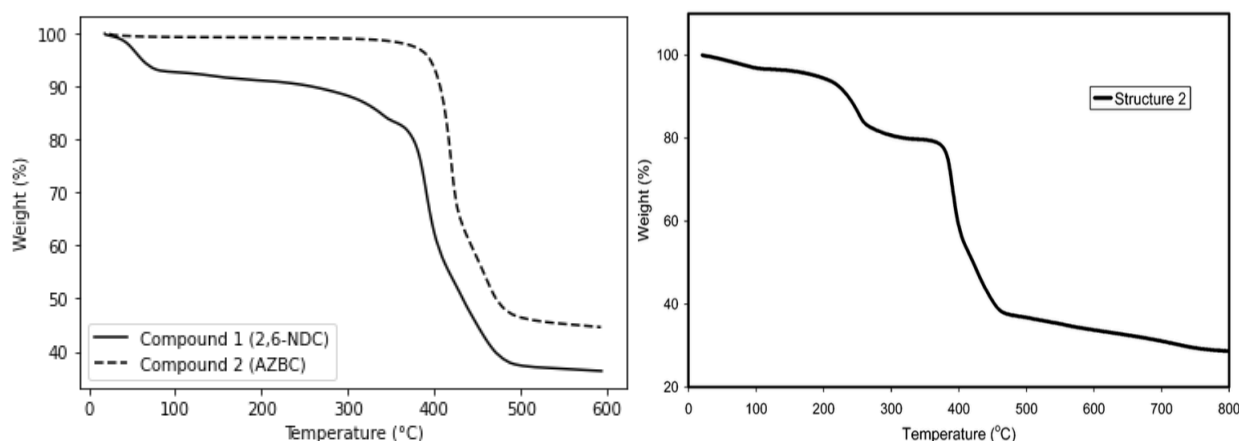


Figure 18. Comparison between TGA curves for both MOFs and reference. R1 thermogram source: (7).

GAS ADSORPTION. BET surface area values of 197.1 m²/g for compound **1** and 18.0 m²/g for compound **2** have been obtained; significantly lower than those obtained for **R1** (584.1 m²/g). As **1** and **R1** are the same MOF, more similar surface area values were expected. The variation between the results may be due to one or more of the following factors: differences in the pretreatment (washing) of the MOF before testing, differences in the quality or accuracy of the used equipment, or differences in the structure of the MOFs resulting from the synthesis. A comparison between the isotherms of **1** and **2** and the isotherms of the compounds synthesized in literature (7) is shown in Figure 19.

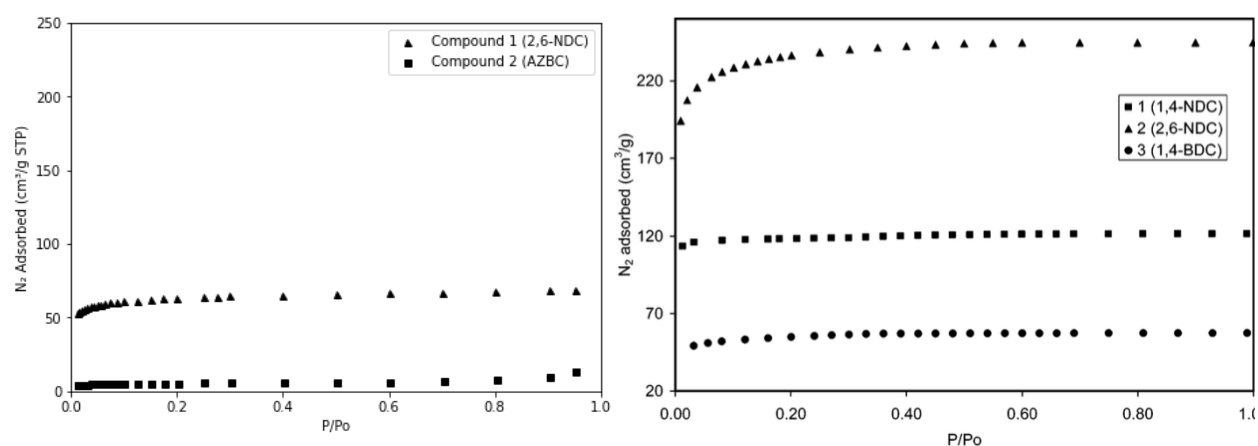


Figure 19. N₂ adsorption curves comparison.

The total pore volume is 0.11 cm³/g at P/P₀=0.95 for compound **1** versus 0.02 cm³/g at P/P₀ = 0.95 for compound **2**, while the average radius is of 22 Å for **1** and of 47 Å for **2**.

The compound **1** isotherm corresponds to an IUPAC Type I isotherm, characteristic of microporous solids (average pore radius < 20 Å) with a relatively small surface area. In this type of material, once the micropores are covered by an initial layer of molecules (monolayer), the surface will have no more space for further adsorption. Therefore, the adsorption process stops, and the material no longer adsorbs, despite the increase in partial vapor pressure.

The isotherm of compound **2** corresponds to an IUPAC Type II isotherm, characteristic of mesoporous (average pore radius between 20 and 50 Å) or non-porous solids. In this case, once a monolayer has formed, the material continues to adsorb, giving rise to multilayers. This type of isotherm is obtained when the affinity of the molecule for the surface is greater than that of the molecule for itself.

In summary, compound **1** has pores at the boundary between micro and meso pores and is a type I isotherm; while compound **2** has pores at the boundary between meso and macro pores and is a type II isotherm. Figures 20(a) and 20(b) show the adsorption isotherms for both MOFs.

Despite being microporous, the specific surface area and total pore volume of **1** is much larger than those of **2**, which explains why, although it does not adsorb molecules beyond the monolayer (being a type I isotherm), it adsorbs almost five times more N₂ than **2**.

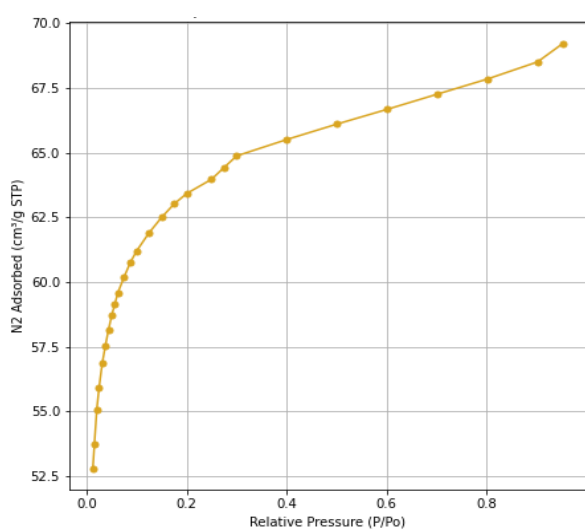


Figure 20(a). Compound 1 N₂ adsorption isotherm.

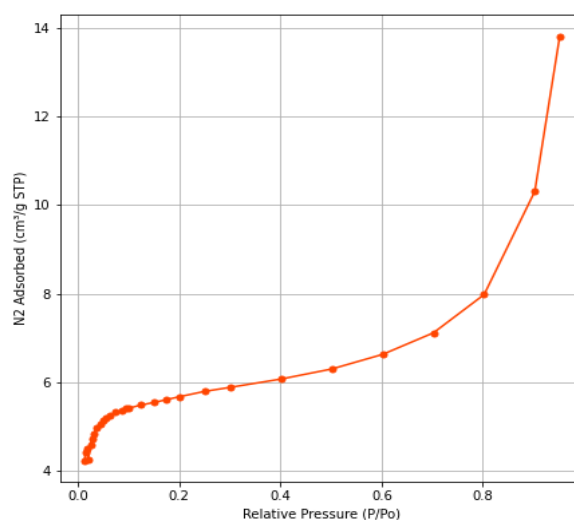


Figure 20(b). Compound 2 N₂ adsorption isotherm.

4.3. ANALYTICAL PERFORMANCE

Figures [21(a)] and [21(b)] show the percentage of analyte extracted and peak area results obtained for **1** and **2**. Figure 22 shows the peak area results for the MOFs synthesized in literature (8), CIM-81, CIM-82, and CIM-83. In cases where there is no error bar, one or two of the results have been discarded for giving anomalous values (e.g., values twice as large as the others obtained in the series or percentage of analyte extracted > 100). Two of the compounds, MPB and OCR, have not been detected in the chromatography, and are not included in the present results.

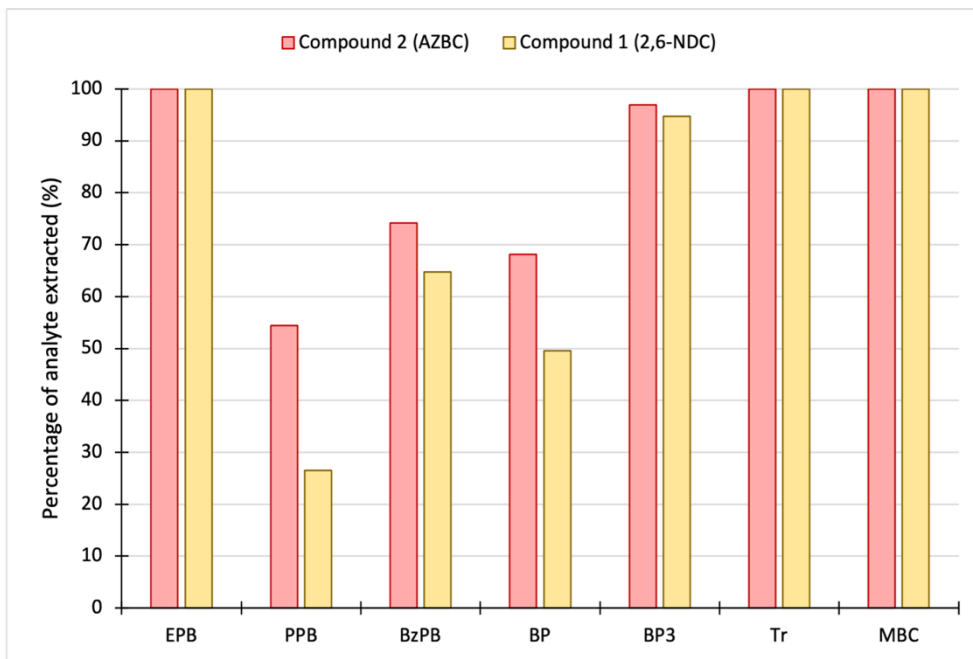


Figure 21(a). Results of percentage of analyte extracted for Compound 1 (2,6-NDC) and Compound 2 (AZBC).

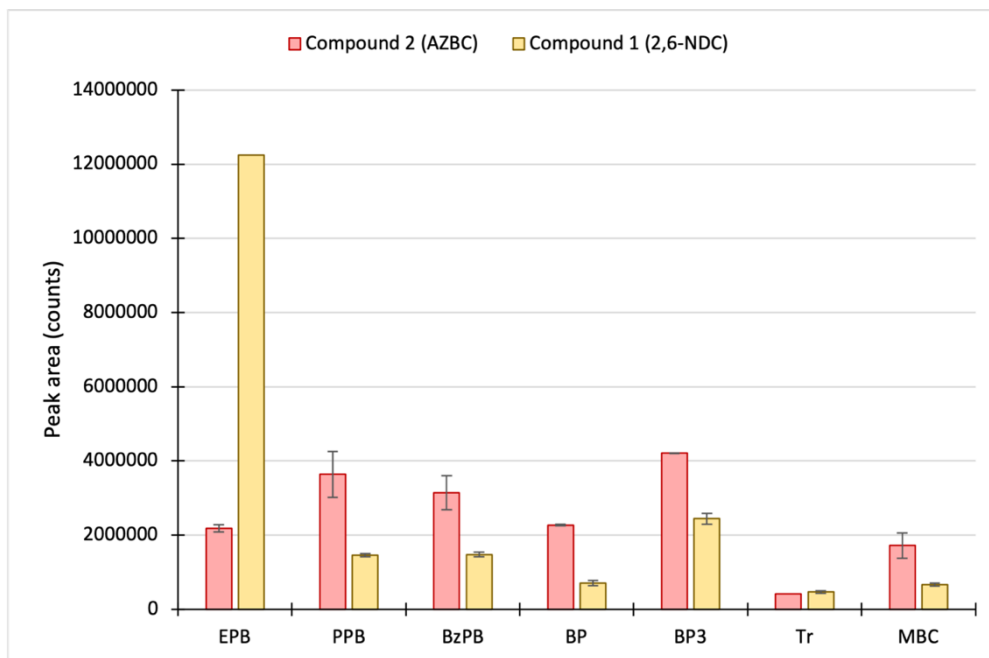


Figure 21(b). Results of peak area for Compound 1 (2,6-NDC) and Compound 2 (AZBC).

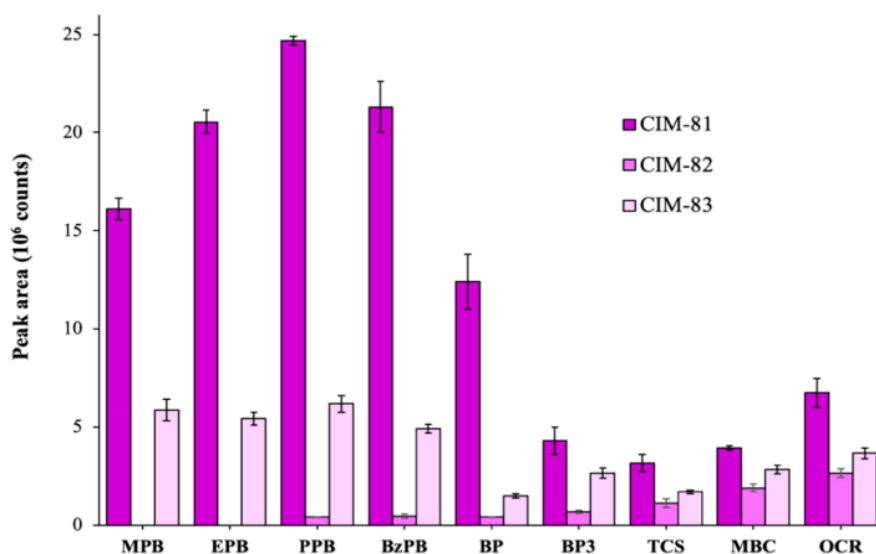


Figure 22. Results of peak area for MOFs synthesized in literature (8).

In the case of **1**, the percentage of analyte extracted is remarkably high in all cases, being practically 100% for EPB, Tr, MBC, and BP3. The adsorption capacities of the remaining compounds, BP, BzPB, and PPB, vary between 55% and 70%.

Compound **2** presents similar results for EPB, Tr, MBC, and BP3 (100%). For the remaining compounds, the results are slightly lower: 65% for BzPB, 50% for PPB, and 30% for BP, almost half that for **1**.

In this respect, both MOFs have a similar behavior: they have the highest capacities for MBC, PPB, and EPB compounds and the lowest for BP, Tr, and BP3. In this sense, the extraction and preconcentration capacities are higher for compounds with lower $\log K_{ow}$ values, lower molecular weight, and a single aromatic ring. This seems to suggest a higher affinity of both compounds for smaller and polar substances.

Regarding the peak area (Figures 21(b) and 22), in the case of **2**, the results are relatively homogeneous, varying between 2E6 and 4E6 counts. The highest peak area is for BP3, followed by PPB, BzPB, BP, MBC, EPB, and Tr. The fact that the peak area results are so similar between compounds whose adsorption capacity is quite different (e.g., the peak area for PPB and BP3 is practically the same, but their adsorption capacities are 55% and 100%, respectively) suggests that MOFs with the highest adsorption capacity have the lowest

desorption capacity and vice versa. Indeed, the compounds that adsorb the most are the ones that will have the highest affinity for the analytes, and, therefore, the ones that will tend to desorb the least. In the case of Tr, this difference is particularly obvious: it adsorbs 100% of the analyte, but hardly desorbs it.

For compound **1**, the peak areas are also relatively similar, higher for BP3 and BzPB and lower for Tr. The peak area of EPB is extraordinarily large (the highest value by far), which does not match the trend shown in the other data as for all the remaining CECs. It is important to mention that **1** has one of the lowest peak area values compared to the rest of the MOFs.

In general, the peak areas obtained with **1** and **2** (between 2E6 and 4E6 counts) are smaller than those obtained with **CIM-81** (between 5E6 and 25E6 counts), similar to those observed for **CIM-82** (between 2E6 and 5E6 counts) and higher than those for **CIM-83** (between 2E6 and 4E6 counts).

Compound **1** has the lowest errors, indicating good reproducibility, and compound **2** errors are significantly higher, especially for EPB, MBC, and PPB. However, for both compounds, the relative error is acceptable.

In general, **1** errors are lower than those of **CIM-81** and similar to those of **CIM-82** and **CIM-83**. The errors of **2** are similar to those of **CIM-81** and **CIM-82** and larger than those obtained for **CIM-83**.

In summary: compound **1** and compound **2** have remarkably high adsorption capacities and medium preconcentration capacities. The results of both extraction and adsorption capacities are similar to those obtained for compound **CIM-82**, synthesized in the literature (8). In general, **1** and **2** demonstrate higher adsorption toward CECs with higher polarity, and lower mass and size molecules, showing the highest performance for EPB, Tr, MBC, and BP3. The results of compound **2** are slightly better than those of compound **1** in terms of extraction capacity, but its standard deviation is higher. However, in both cases, the relative error seems to indicate a good reproducibility of the experiment. Overall, the results seem to indicate that both compounds have good potential as extractants of contaminants.

CONCLUSIONS

En esta sección se resumen los resultados obtenidos. Se han logrado sintetizar y caracterizar ambos MOFs con éxito. Los resultados del screening señalan a ambos MOFs como buenos extractores de contaminantes. Tras comparar los resultados con la literatura, se concluye que tienen un rendimiento parecido a los de otros MOFs de la misma familia.

Two pillared-layer MOFs were successfully synthesized and characterized. The MOFs were composed by layers formed by Zn(II) metal ions and TRZ motifs, linked by two different aromatic dicarboxylates: 2,6-NDC for compound **1** and azobenzene AZBC for compound **2**.

According to the X-ray diffraction, the synthesized MOFs have a high crystalline quality. Both **1** and **2** are thermally stable up to 300 °C and lose, in total, about 50% of their mass, with **2** starting to decompose the latest and being the most stable overall. From the gas adsorption test, it has been found that **1** behaves as a microporous solid and has a specific surface area 100 times higher than compound **2**.

Compound **1** has been compared with the literature (7) and very similar results have been found in the thermal analysis and X-ray diffraction results, which points towards a correct synthesis of the MOF. In the gas adsorption test, however, the results have been significantly different: the specific surface area of the synthesized MOF is practically half than that reported in the literature (7).

The synthesized MOFs were applied in a μ -dSPE approach to evaluate their efficiency as extractants of a group of CECs. Both MOFs demonstrate excellent adsorption capacity for most compounds. The results are, in general, slightly better for compound **2** than for compound **1**. Comparing the peak area results with those in the literature (8), it can be concluded that both compound **1** and compound **2** have a similar extraction capacity to **CIM-82**, and that, in general, they have the potential to compare favorably. In any case, further analytical experiments with both MOFs are needed to obtain more accurate results, and to establish more definitive conclusions regarding their ability as sorbents in μ -dSPE.

REFERENCES

- (1) Francisco G Calvo-Flores, Joaquín Isac-García, and José A Dobado Jiménez - *Emerging pollutants: origin, structure, and properties* (2018)
- (2) Hongkai Zhu, Kurunthachalam Kannan - *Parabens in stretch mark creams: A source of exposure in pregnant and lactating women* (2020)
- (3) Teddy Kabeya Kasonga, Martie A. Coetzee, Ilunga Kamika, Veronica M Ngole-Jeme, Maggy Ndombo Benteke Momba - *Endocrine-disruptive chemicals as contaminants of emerging concern in wastewater and surface water: A review* (2020)
- (4) Shweta Sharma - *Contaminants of Emerging Concern - A Review* (2014)
- (5) Illinois-Indiana Sea Grant - *Contaminants of Emerging Concern* (2019)
- (6) Brandon Chuan Yee Lee, Fang Yee Lim, Wei Hao Loh, Say Leong Ong and Jiangyong Hu - *Emerging Contaminants: An Overview of Recent Trends for Their Treatment and Management Using Light-Driven Processes* (2021)
- (7) Hyunsoo Park, James F. Britten, Ulrich Mueller, JeongYong Lee, Jing Li, and John B. Parise - *Synthesis, Structure Determination, and Hydrogen Sorption Studies of New Metal-Organic Frameworks Using Triazole and Naphthalenedicarboxylic Acid* (2006)
- (8) Providencia González-Hernández, Adrián Gutiérrez-Serpa, Ana B. Lago, Laura Estévez, Juan H. Ayala, Verónica Pino, and Jorge Pasán - *Insights into Paraben Adsorption by Metal-Organic Frameworks for Analytical Applications* (2021)
- (9) Providencia González-Hernández, Ana B. Lago, Jorge Pasán, Catalina Ruiz-Pérez, Juan H. Ayala, Ana M. Afonso and Verónica Pino - *Application of a Pillared-Layer Zn-Triazolate Metal-Organic Framework in the Dispersive Miniaturized Solid-Phase Extraction of Personal Care Products from Wastewater Samples* (2019)
- (10) Xiao-Li Hu, Qi-Han Gong, Rong-Lin Zhong, Prof. Xin-Long Wang, Prof. Chao Qin, Hao Wang, Prof. Jing Li, Kui-Zhan Shao, Prof. Zhong-Min Su - *Evidence of Amine-CO₂ Interactions in Two Pillared-Layer MOFs Probed by X-ray Crystallography* (2015)

(11) Quan-Guo Zhai, Ni Bai, Shu'ni Li, Xianhui Bu, and Pingyun Feng - *Design of Pore Size and Functionality in Pillar-Layered Zn-Triazolate-Dicarboxylate Frameworks and Their High CO₂/CH₄ and C₂ Hydrocarbons/CH₄ Selectivity* (2015)

(12) Yitong Han, Hong Yang and Xinwen Guo - *Synthesis Methods and Crystallization of MOFs* (2019)

(13) Aysha Alobeidli, Haifa Ben Salah, Mohammed Al Murisi, Rana Sabouni - *Recent advancements in MOFs synthesis and their green applications* (2021)

(14) Sopan N. Nangare Pravin O. Patil Ashwini G. Patil Sachin M. Chandankar - *Nanostructured metal-organic framework-based luminescent sensor for chemical sensing: current challenges and future prospects* (2022)

(15) Augustus Newton Ebelegi, Ayawei Nimibofa, Azibaola Kesiye Inengite, Wankasi Donbebe - *Metal-organic Frameworks as Novel Adsorbents: A Preview* (2017)

(16) Yi Luo¹, Saientan Bag, Orysia Zaremba, Jacopo Andreo, Stefan Wuttke, Pascal Friederich, and Manuel Tsotsala - *MOF Synthesis Prediction Enabled by Automatic Data Mining and Machine Learning*

(17) Wajid Ali Khan, Muhammad Balal Arain, Yadollah Yaminic, Nasrullah Shaha, Tasneem Gul Kazi, Stig Pedersen-Bjergaard, and Mohammad Tajikc - *Hollow fiber-based liquid phase microextraction followed by analytical instrumental techniques for quantitative analysis of heavy metal ions and pharmaceuticals* (2020)

(18.1), (18.2), (18.3), (18.4), (18.5), (18.6), (18.7), (18.8), (18.9) PubChem pages for methylparaben, ethylparaben, propylparaben, butylparaben, triclosan, octocrylene, and camphor.

(19) Leila Abylgazina, Irena Senkovska, Richard Engemann, Sebastian Ehrling, Tatiana E. Gorelik, Negar Kavooosi, Ute Kaiser, and Stefan Kaskel - *Impact of Crystal Size and Morphology on Switchability Characteristics in Pillared-Layer Metal-Organic Framework DUT-8(Ni)* (2021)

(20) James Campbell, Begum Tokay - *Controlling the size and shape of Mg-MOF-74 crystals to optimise film synthesis on alumina substrates* (2017)

(21) R. Seetharaj, P.V. Vandana, and P. Arya - *Dependence of solvents, pH, molar ratio and temperature in tuning metal organic framework architecture (2016)*